

Numerical Simulation of Two Phase Flow in Reconstructed Pore Network Based on Lattice Boltzmann Method

Song Rui¹, Liu Jianjun^{1,2}, Qin Dahui¹

1, School of Civil Engineering and Architecture, Southwest Petroleum University, Chengdu, China;

2, State Key Laboratory of Oil and Gas Reservoir Geology and Exploitation (Southwest Petroleum University), Chengdu, China;

Abstract

Accurate prediction and understanding of the disorder microstructures in the porous media contribute to acquiring the macroscopic physical properties such as conductivity, permeability, formation factor, elastic moduli etc. Based on the rock serial sectioning images of Berea sandstone acquired by the core scanning system developed by our research group, the reconstructed rock model is established in the Mimics software and the extracted pore network of the porous rock is accomplished by the self-programming software in C++ programming language based on the revised Medial axis based algorithm and the Maximal ball algorithm. Using a lattice Boltzmann method, the single and two – phase flow are accomplished. Both of the pore-scale networks and the seepage mechanism of the single- and two –phase flow are identical with the benchmark experimental data.

Keywords: Berea sandstone; serial sectioning; reconstructed porous media; extracted network; single - phase flow; two – phase flow.

1. Introduction

Accurate prediction and understanding of the disorder microstructures in the porous media, such as rocks [1], soils [2], biomedical field [3], ceramics [4], and composites [5], contribute to acquiring the macroscopic physical properties such as conductivity, permeability, formation factor, elastic moduli etc. [6 - 8]. Though those transport properties can be obtained by experiments, it is hard to gain the detailed information of the fluid flow in the pore and to conduct the three – phase flow experiment in the current conditions.

The pore-scale network model describing the disorder system in the porous media is considered as a starting point emphasized by many scholars [9-12]. Fortunately, with the developing of electronic computer and the technology of porous media imaging in recent years, such as Scanning Electron Microscopy (SEM)[13,14], serial sectioning[15-17], confocal laser scanning microscopy[18], micro X-ray computerized tomography (micro-CT)[19]and reconstructed porous media by mathematical methods[1,20], it is applicable to acquire the pore space images mapping the real interior structure of its original

sample, on basis of which the pore-scale numerical simulation can be carried on to make the above study complete. However, it is necessary to develop an effective algorithm to extract the pore network from these three dimensional porous media. In this paper, based on the rock serial sectioning images of Berea sandstone acquired by the core scanning system developed by our research group, the reconstructed rock model is established in the Mimics software and the extracted pore network of the porous rock is accomplished by the self-programming software in C++ programming language based on the revised Medial axis based algorithms [21-22] and the Maximal ball algorithm [23-24]. Using a lattice Boltzmann method, the single and two – phase flow are accomplished. Both of the pore-scale networks and the seepage mechanism of the single- and two –phase flow are identical with the benchmark experimental data.

2. Reconstructed Berea Sandstone and the Extracted Pore Network Model

2.1 Serial Sectioning Imaging of the Berea Sandstone and Reconstructed Model

Serial sectioning provides a direct way to visualize 3D microstructures when successive layers of materials are removed and exposed surfaces are imaged at high resolution. The 3D image of pore media can be obtained by stacking serial sections [25]. The workflow of the serial sectioning is illustrated in Fig.1.

In this paper, the images of the Berea sandstone section are obtained by the self – developed core scanning system. The rock matrix and the pore space are identified using the optical properties of different minerals in the scanning system, the cell size is $3.45 \mu m \times 3.45 \mu m$ for the maximum resolution of 2454 Pixel \times 2056 Pixel. For the sake of the storage space increasing sharply along with the resolution and the feasibility of the numerical simulation, the image resolution for this paper is $9 \mu m$, in which case the storage space of the reconstructed

sandstone is 1.2GB and the extracted pore network is 526 MB. Fig.2 shows two of the sandstone slice images using

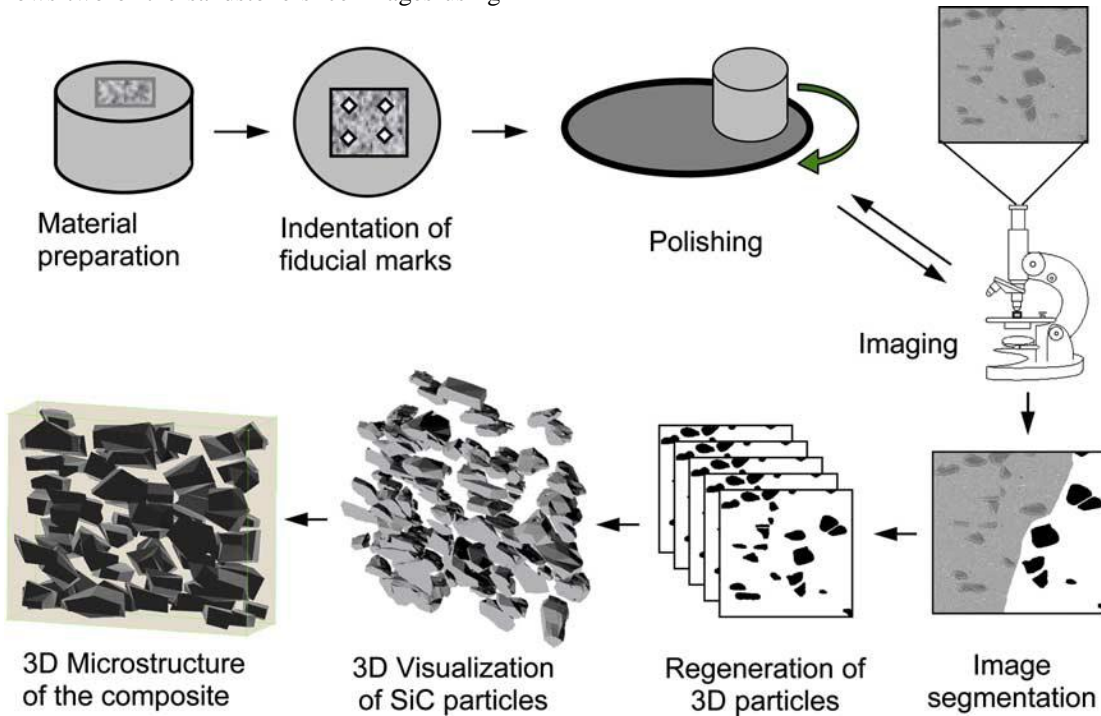


Figure 1. Flow chart of serial sectioning and 3D reconstruction process [25].

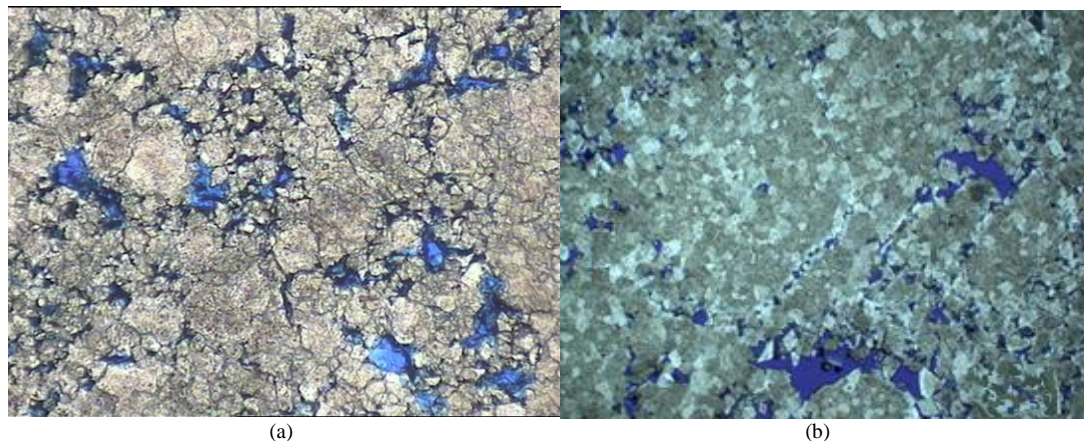


Figure 2. The sandstone slice images

Berea sandstone is selected as the original sample, and a total of 97 sections are polished in this study. And the central part of the images for 300 Pixels \times 300 Pixels is selected as the basic data to reconstruct the porous media. Due to being storage individually, as a result of which the image data is discrete, these images are imported into the ImageJ software by the National Institutes of Health in sequence. Then Binary images are obtained by utilizing the information of shadow of stone and

the gray image histogram of the origin SEM image, by which the rock matrix and the pore space can be resolved from the white part and the black, respectively. Followed that, the images are de-noised and smoothed and converted into the standard CT format (.raw) in ImageJ. Four of the processed images are shown in Fig.3. Finally, the images data with a .raw suffix is imported into Mimics software to accomplish the reconstructed Berea sandstone model, the size of which is 2700 μ m \times 2700 μ m \times 2700 μ m in Fig.4.

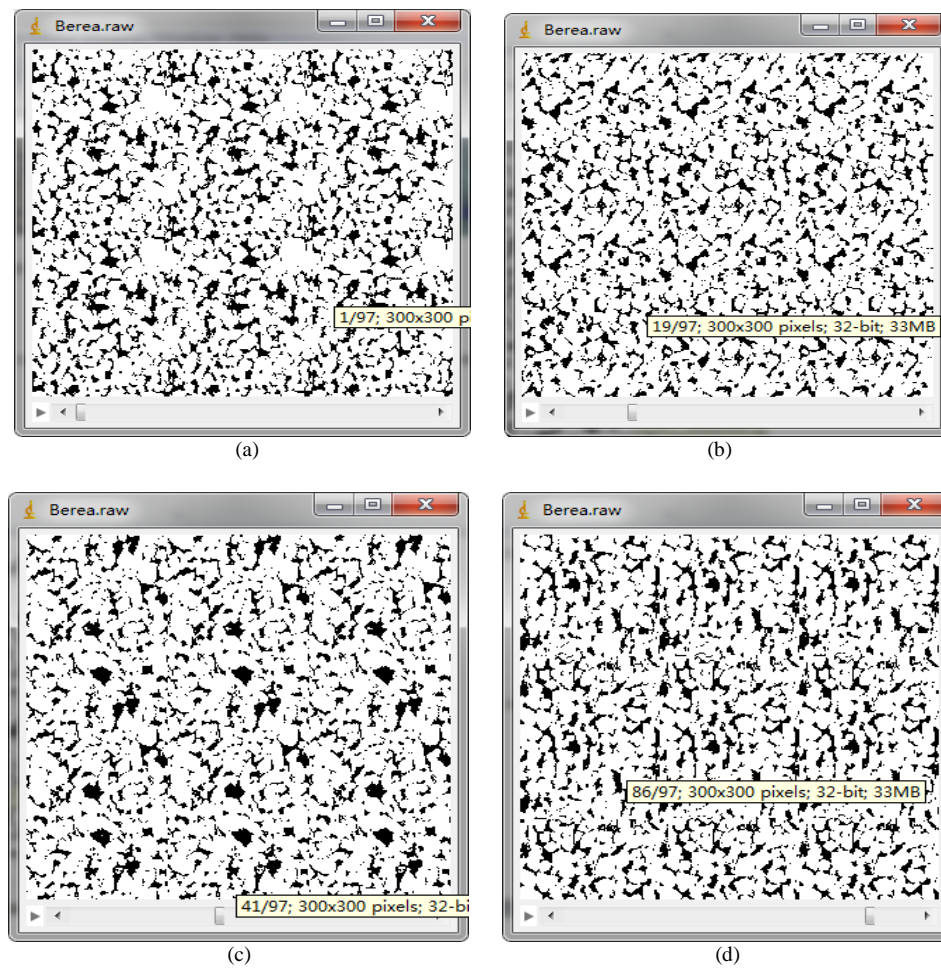


Figure 3. The processed sandstone images (300 Pixels × 300 Pixels). The white part is the rock matrix and the black part is the pore space. (a) is the top image of the 97; (b) is the 19th; (c) is the forty-first; (d) is the 86th.

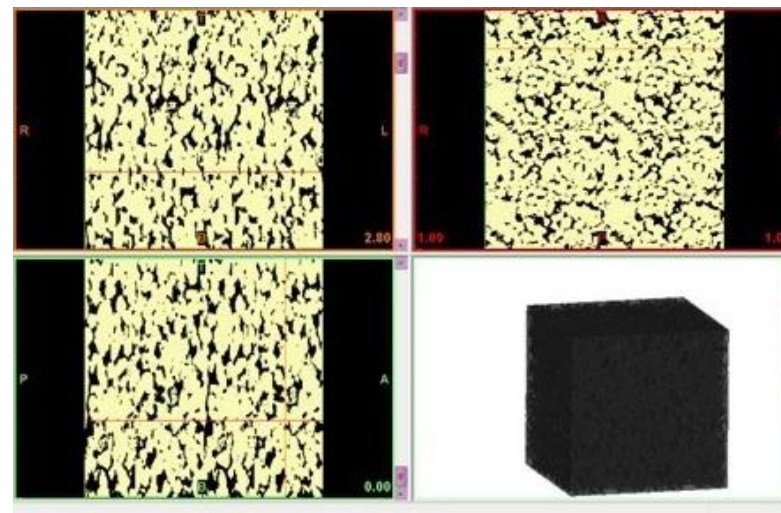


Figure 4. The three view of the reconstructed Berea sandstone and the three – dimensional model in Mimics software.

2.2 Extracted Pore Network of the Reconstructed Berea Sandstone Model

As established in the previous section, the three-dimensional porous media can be acquired in many ways. However, for further study on the transport properties in the porous media, it is essential to develop an effective algorithm to extract the pore network of the three-dimensional porous media images, which is considered as a breakthrough point by many scholars. The synthetical and revised pore network algorithm evaluated from the Medial axis based algorithm and the Maximal ball algorithm, the workflow of which is as follows:

1. The three – dimensional porous media image is segmented and exported as the txt image, the maximum RGB value of which is limited as 1, that is 0 represents the pore space and 1represents the rock matrix. Each number represents a voxel in the image. Part of the txt image is shown in the Fig.5.

2. Along the status “0” in the txt image the medial axis will be obtained and located accurately, that is, the center of the pore is known. Taking the central point as the center of sphere, the sphere is expanded until touching the rock matrix voxel. Then every sphere is numbered according with the radius of the sphere.

3. The largest ball is defined as pore, then the second. The connected balls form pore chains, and the ball where the two different chains meets are defined as throat and replace by the cylinder with the same radius.

4. The same sorting processes are applied for all the ball chains until reaching the minimum size set for a pore in our self-programming system. Below this threshold, the ball may provide connections (be throats) but cannot be pores.

Based on the theory above, we develop the pore network extraction system and provide visualization model in Rhinoceros software, and complete the pore network and one of the cross sections of the model shown in the Fig.6. The geometrical parameters are listed in the table 1, by which we can find the algorithm is feasible.

Figure 5. The txt image of the porous media

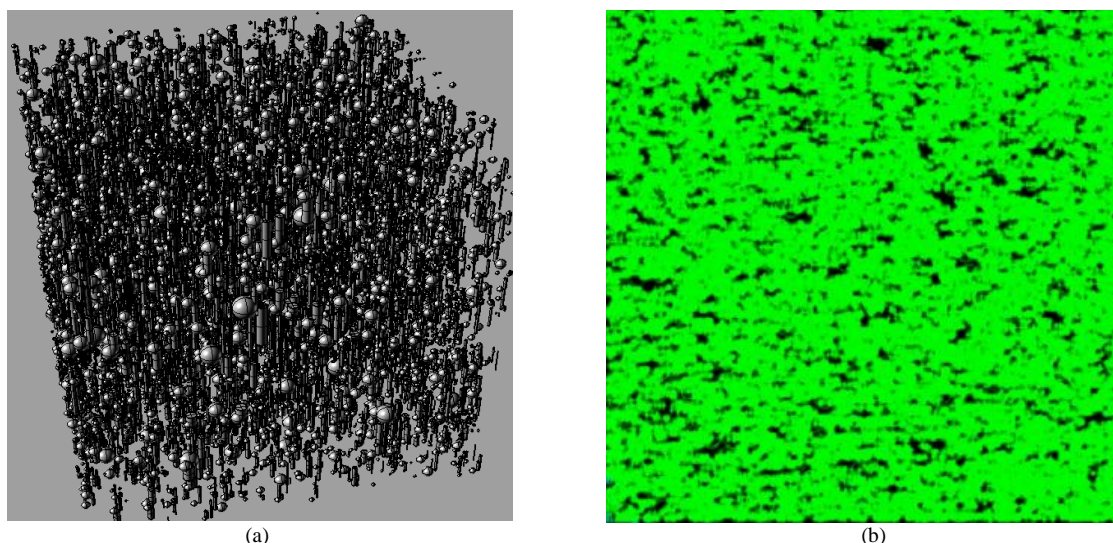


Figure 6. The extracted pore network. (a) is model in Rhinoceros software; (b) is the one of the cross sections of the model.

Table 1. The geometrical parameters of the extracted pore network

| Geometrical Parameters | Count or Size |
|---------------------------------|---------------|
| Porosity | 14.06% |
| Number of the Pores | 1868 |
| Number of the throat | 3053 |
| Average connection number | 3.15685 |
| Minimum connection number | 0 |
| Maximum connection number | 12 |
| Number of connections to inlet | 124 |
| Number of connections to outlet | 138 |
| Average pore radius | 19.04 μ m |
| Average throat radius | 7.29 μ m |

3. Numerical study on the extracted pore network based on lattice Boltzmann method

To verify the feasibility of our pore network extraction algorithm, the single – and two – phase flow experiment and simulation study are conducted in this study. For the sake of the disconnection of different pore chains, it is impossible to be meshed in the commercial FEM software. Unlike conventional numerical schemes based on discretizations of macroscopic continuum equations, the lattice Boltzmann method is based on microscopic models and mesoscopic kinetic equations. The fundamental idea of the LBM is to construct simplified kinetic models that incorporate the essential physics of microscopic or mesoscopic processes so that the macroscopic averaged properties obey the desired macroscopic equations [26-29].

Single-phase flow is simulated across the extracted network and the absolute permeability is calculated on the network by the self-programming software in C++ programming language using Lattice Boltzmann and compared to the experimental absolute permeability results on the same rock sample.

3.1 Mathematical model for flow in the pore network using lattice Boltzmann method

The absolute permeability K of the network is derived from Darcy's law [10]:

$$K = \frac{\mu_p q_{tsp} L}{A(\Phi_{inlet} - \Phi_{outlet})} \quad (1)$$

where the network is fully saturated with a single phase p of viscosity μ_p ; q_{tsp} is the total single phase flow rate through the pore network of length L with the potential drop $(\Phi_{inlet} - \Phi_{outlet})$. A is the cross-sectional area of the model.

Then relative permeability is

$$k_{rp} = \frac{q_{tmp}}{q_{tsp}} \quad (2)$$

where q_{tmp} is the total flow rate of phase p in multiphase conditions with the same imposed pressure drop.

The conductance of the single phase g_p is given by the Hagen-Poiseuille formula:

$$g_p = k \frac{A^2 G}{\mu_p} \quad (3)$$

For a circular, an equilateral and a square tube, the constant k is 0.5, 0.6 and 0.5623 respectively.

The conductance between two pore bodies (i, j) via throat (t) is given as:

$$\frac{l_{ij}}{g_{p,ij}} = \frac{l_i}{g_{p,i}} + \frac{l_t}{g_{p,t}} + \frac{l_j}{g_{p,j}} \quad (4)$$

where l_{ij} is the distance from pore i center to pore j center (throat total length); l_i and l_j are the pore body lengths which are the lengths from the pore-throat interface to the pore centers, as illustrated in Fig. 7

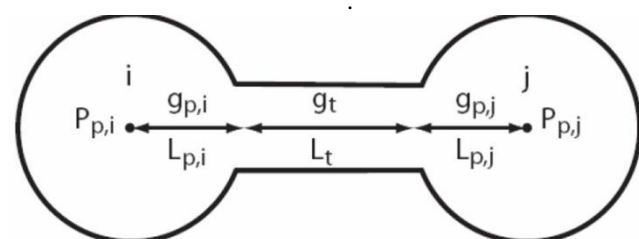


Figure 7. Conductance between two pores [30].

The lattice Boltzmann equation is:

$$f_i(\vec{x} + \vec{e}_i, t+1) - f_i(\vec{x}, t) = \frac{I}{t}(f_i^0 - f_i) \quad (5)$$

where $f_i(\vec{x}, t)$ is the particle distribution function at location x and time t along the i th direction ($i=0,1,2\dots 18$)

using three-dimensional nineteen velocity model and where τ is the single time relaxation parameter and f_i^o is the local equilibrium state depending on the local density and velocity [26].

3.2 Comparison between the experimental results and the simulation

The comparison between the experimental results and the simulation can be seen in the table 2, by which we can find the porosity and the absolute permeability of the extracted pore network is quite close to the benchmark experimental data for the same Berea sandstone sample. In

the same way, the relative permeability curve for the two – phase flow in the extracted pore network and the experiment is shown in the Fig.8. These indicate that, even though the micro structure, which may be in different geological shapes, is substituted by the balls and cylinder, the extracted network approaches to the microstructure in the origin sample for the size of $2.7 \text{ mm} \times 2.7 \text{ mm} \times 2.7 \text{ mm}$, which verifies that the extraction algorithm and the simulation software developed by our group is feasible and applicable in the porous media study.

Table 2. Single – phase flow result of the experiment and the simulation

| Method | Porosity | Absolute permeability |
|------------|----------|-----------------------|
| Experiment | 14.53% | 1633.52md |
| Simulation | 14.06% | 1752.18md |

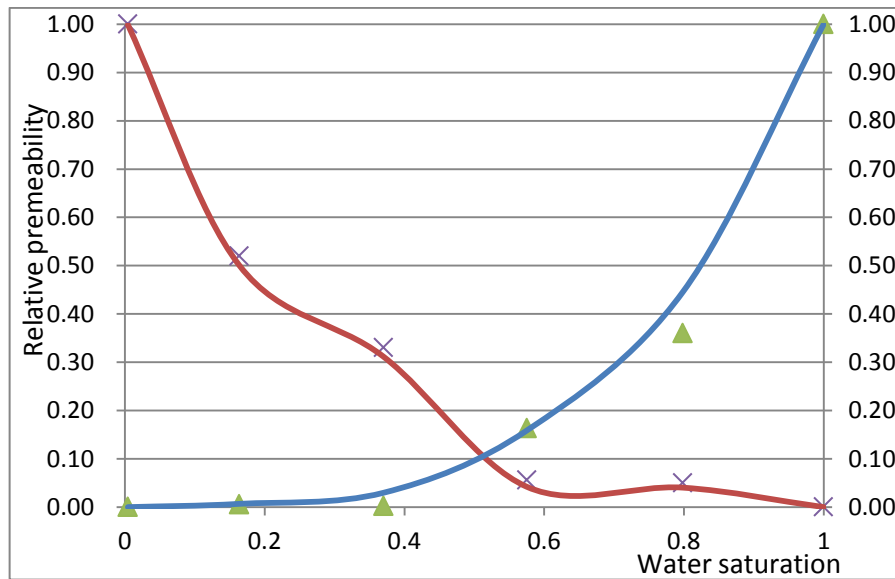


Figure 8. Relative permeability vs. water saturation; the splashes are experimental results while the curves are the simulation.

4. Conclusion

In this paper, an effective method of reconstructing the three - dimensional model from the serial sectioning image of Berea sandstone and an effective pore network extraction algorithm is presented. Using the lattice Boltzmann method, the single and two – phase flow are accomplished. Both of the pore-scale networks and the seepage mechanism of the single- and two –phase flow are identical with the benchmark experimental data. The study aims to provide an ideal pore network model describing the same microstructure of the origin sample, and apply the network to numerical simulation. In future, we will

develop the visualized distribution cloud chart of the different fluid for the multi – phase flow to make the study more reliable and applicable.

Acknowledgement

This paper is financially supported by Natural Science Foundation of China (Grant No.51174170) and National Science and Technology Major Project of China under Grant No. 2011ZX05013-006.

Reference

- [1] D. Bauer, S. Youssef, M. Fleury, S. Bekri, E. Rosenberg, O. Vizika, Improving the Estimations of

- Petrophysical Transport, *Transp Porous Med* 94, 2012, pp.505–524.
- [2] M. Kataja, K. Hiltunen, and J. Timonen, *J. Phys. D* 25, 1992, 1053.
- [3] Zollakofer Christoph P.E. et al. Tools for rapid prototyping in the biosciences. *IEEE Computer Graphics and Applications*, 12, 1995, pp.48-57.
- [4] H. Kamiya, K. Isomura, G. Jimbo, and T. Jun-ichiro, *J. Am.Chem. Soc.* 78, 49, 1995.
- [5] Michele Panico. Modeling of Shape Memory Alloys and Application to Porous Materials. PHD thesis, NORTHWESTERN UNIVERSITY, EVANSTON, ILLINOIS , 2008.
- [6] R. Hilfer and Th. Zauner. High-precision synthetic computed tomography of reconstructed porous media, *PHYSICAL REVIEW E* 84, 062301, 2011.
- [7] Blunt, M.J.. Flow in porous media pore-network models and multiphase flow. *Current Opinion in Colloid & Interface Science*, 6, 2001, pp. 197-207
- [8] D.Bauer, S.Youssef, M. Fleury, S. Bekri, E.Rosenberg, O. Vizika. Improving the Estimations of Petrophysical Transport Behavior of Carbonate Rocks Using a Dual Pore Network Approach Combined with Computed Microtomography. *Transp Porous Med*, 94, 2012, pp.505–524.
- [9] R. Elliot, J. Krumhansl, and P. Leath, The theory and properties of randomly physical systems, *Rev. Mod. Phys.*, vol. 46, no. 3, pp. 465-543, 1974
- [10] Hu Dong. Micro-CT imaging and pore network extraction. PhD thesis, Imperial College London, 2007.
- [11] B. Biswal, P.-E. Øren, R. J. Held, S. Bakke, and R. Hilfer. Stochastic multiscale model for carbonate rocks. *PHYSICAL REVIEW E* 75, 061303, 2007.
- [12] Wenddabo Olivier Sawadogo, Noureddine Alaa, Blaise Somé Numerical simulation of groundwater level in a fractured porous medium and sensitivity analysis of the hydrodynamic parameters using grid computing: application of the plain of Gondo (Burkina Faso). *International Journal of Computer Science Issues*, v 9, n 1 1-2, 2012, p 227-236.
- [13] McMullan, D. Von Ardenne and the scanning electron microscope. *Proc Roy Microsc Soc* 23, 1988, pp.283-288.
- [14] 14. McMullan, D. Scanning electron microscopy 1928–1965. *Scanning* 17, 1995, pp.175–185.
- [15] Lymberopoulos, D.P. and Payatakes, A.C. Derivation of topological, geometrical, and correlational properties of porous media from pore-chart analysis of serial section data. *Journal of Colloid and Interface Science*, 150(1):61-80, doi: 10.1016/0021-9797(92)90268Q, 1992.
- [16] Vogel, H.-J. Roth, K. Quantitative morphology and network representation of soil pore structure. *Advances in Water Resources* 24(3-4), 2001, pp. 233-242.
- [17] Tomutsa, L. and Silin, D.. Nanoscale Pore Imaging and Pore Scale Fluid Flow Modeling in Chalk. Lawrence Berkeley National Laboratory: Paper LBNL56266 (2004).
<http://repositories.cdlib.org/lbnl/LBNL-56266>.
- [18] Fredrich, J.T., Menendez, B. and Wong, T.-F. Imaging the pore structure of geomaterials. *Science*, 268, 1995, pp. 276-279.
- [19] Dunsmuir, J.H., Ferguson, S.R., D'Amico, K.L. and Stokes, J.P. X-ray microtomography: a new tool for the characterization of porous media, Paper SPE 22860, Proceedings of 66th Annual Technical Conference and Exhibition of the Society of Petroleum Engineers, Dallas, TX (1991).
- [20] D.Bauer, S.Youssef, M. Fleury, S. Bekri, E.Rosenberg, O. Vizika. Improving the Estimations of Petrophysical Transport Behavior of Carbonate Rocks Using a Dual Pore Network Approach Combined with Computed Microtomography. *Transp Porous Med*, 94, 2012, pp.505–524.
- [21] Lindquist, W.B., Lee, S.M., Coker, D., Jones, K. and Spanne, P. Medial axis analysis of void structure in three-dimensional tomographic images of porous media. *Journal of Geophysical Research*, 101B: 8297, 1996.
- [22] Lindquist, W.B. and Venkatarangan, A. Investigating 3D Geometry of Porous Media from High Resolution Images. *Phys. Chem. Earth (A)*, 25(7), 1999, pp. 593-599.
- [23] Silin, D. and Patzek, T. Pore space morphology analysis using maximal inscribed spheres. *Physica A*, 371, 2006, pp. 336-360.
- [24] Silin, D.B., Jin, G. and Patzek, T.W. Robust Determination of Pore SpaceMorphology in Sedimentary Rocks, Paper SPE 84296, Proceedings of SPE Annual Technical Conference and Exhibition, Denver, Colorado, U.S.A, 2003.
- [25] Chawla, N., Sidhu, R.S. and Ganesh, V.V. Three-dimensional visualization and microstructure-based modeling of deformation in particle-reinforced composites. *Acta Materialia*, 54(6), 2006, pp.1541-1548.
- [26] Shiyi Chen, Gary D. Doolen. LATTICE BOLTZMANN METHOD FOR FLUID FLOWS. *Annu. Rev. Fluid Mech.* 30, 1998, pp.329–64.
- [27] Dyntar, Jakub, Soucek, Ivan; Gros, Ivan. Application of discrete event simulation in LPG storage operation and optimization. *International Journal of Computer Science Issues*, v 9, n 3, 2012, pp. 33-42.
- [28] Rastaghi, Roohallah,); Oskouei, Hamid R. Dalili. Cryptanalysis of a public-key cryptosystem using lattice basis reduction algorithm. *International*

- Journal of Computer Science Issues, v 9, n 5 5-1,
2012, pp. 110-117.
- [29] Rakhshani, Mohammad Reza, Mansouri-Birjandi,
Mohammad Ali. Design and optimization of photonic
crystal triplexer for optical networks. International
Journal of Computer Science Issues, v 9, n 4 4-1,
2012, pp. 24-28.
- [30] Valvatne, P.H. Predictive pore-scale modelling of
multiphase flow. PhD thesis, Department of Earth
Science and Engineering, Imperial College London,
2004.